Stem Cell Research (2014) 13, 240–250

Available online at www.sciencedirect.com

ScienceDirect

www.elsevier.com/locate/scr

FANCA knockout in human embryonic stem cells causes a severe growth disadvantage

Kim Vanuytsel[a,*], Qing Cai[a], Nisha Nair[a], Satish Khurana[a], Swati Shetty[a], Joris R. Vermeesch[b], Laura Ordovas[a,1], Catherine M. Verfaillie[a,1]

[a] *KU Leuven Stem Cell Institute, Department of Development and Regeneration, Cluster Stem Cell Biology and Embryology, Herestraat 49, Onderwijs en Navorsing 4, Box 804, 3000 Leuven, Belgium*
[b] *KU Leuven Center for Human Genetics, 3000 Leuven, Belgium*

Received 8 April 2014; received in revised form 16 July 2014; accepted 20 July 2014
Available online 27 July 2014

Abstract Fanconi anemia (FA) is an autosomal recessive disorder characterized by progressive bone marrow failure (BMF) during childhood, aside from numerous congenital abnormalities. FA mouse models have been generated; however, they do not fully mimic the hematopoietic phenotype. As there is mounting evidence that the hematopoietic impairment starts already in utero, a human pluripotent stem cell model would constitute a more appropriate system to investigate the mechanisms underlying BMF in FA and its developmental basis. Using zinc finger nuclease (ZFN) technology, we have created a knockout of *FANCA* in human embryonic stem cells (hESC). We introduced a selection cassette into exon 2 thereby disrupting the *FANCA* coding sequence and found that whereas mono-allelically targeted cells retain an unaltered proliferation potential, disruption of the second allele causes a severe growth disadvantage. As a result, heterogeneous cultures arise due to the presence of cells still carrying an unaffected *FANCA* allele, quickly outgrowing the knockout cells. When pure cultures of *FANCA* knockout hESC are pursued either through selection or single cell cloning, this rapidly results in growth arrest and such cultures cannot be maintained. These data highlight the importance of a functional FA pathway at the pluripotent stem cell stage.

Introduction

Fanconi anemia (FA) is an autosomal recessive disease characterized by congenital abnormalities and progressive bone marrow failure (BMF) in the first decades of life, which develops into hematologic malignancies in 33% of cases (Kutler et al., 2003; Auerbach, 2009). The high cancer predisposition and hypersensitivity to cross-linking agents (Sasaki and Tonomura, 1973; Ishida and Buchwald, 1982; Auerbach et al., 1989), used as a diagnostic criterion, reflect the genomic instability of these patients and illustrate the link with DNA repair processes. FA results from mutations in any of the 16 genes linked together in the FA pathway (*FANCA*, *FANCB*, *FANCC*, *FANCD1*, *FANCD2*,

Abbreviations: FA, Fanconi anemia; BMF, bone marrow failure; ZFN, zinc finger nucleases; hESC, human embryonic stem cells; DSB, double strand breaks; HR, homologous recombination; NHEJ, non-homologous end-joining; HSPC, hematopoietic stem and progenitor cells; WT, wild type; KD, knockdown; RNAi, RNA interference; hiPSC, human induced pluripotent stem cells; MEF, mouse embryonic fibroblasts; FF, feeder-free; bFGF, basic fibroblast growth factor; ROCK, rho-associated proteine kinase; Puro cassette, Puromycin resistance cassette; Hygro cassette, Hygromycin resistance cassette; aCGH, array comparative genomic hybridization; HA, homology arms; SB, Southern blot; ATM, ataxia telangiectasia mutated.

* Corresponding author at: KU Leuven Stem Cell Institute, Herestraat 49, Onderwijs en Navorsing 4, Box 804, 3000 Leuven, Belgium.
E-mail address: kim.vanuytsel@med.kuleuven.be (K. Vanuytsel).
[1] LO and CMV contributed equally as last authors.

http://dx.doi.org/10.1016/j.scr.2014.07.005
1873-5061/

FANCE, *FANCF*, *FANCG*, *FANCI*, *FANCJ*, *FANCL*, *FANCM*, *FANCN*, *FANCO*, *FANCP*, *FANCQ*) (Garaycoechea and Patel, 2014). This pathway is activated upon detection of DNA damage to help resolve stalled replication forks at double strand breaks (DSB) and promote faithful DNA repair through homologous recombination (HR) (Kee and D'Andrea, 2010; Adamo et al., 2010; Pace et al., 2010). When the FA pathway is disrupted, DSB are no longer diverted away from the more error-prone non-homologous end-joining (NHEJ) repair pathway in favor of HR, which likely results in the acquisition of cytogenetic abnormalities (Adamo et al., 2010; Pace et al., 2010; Blanpain et al., 2011).

It is well understood that cytogenetic abnormalities underlie events such as leukemic transformation (Look, 1997). Insights on how accumulation of DNA damage contributes to progressive BMF, however, have only recently started to emerge (Niedernhofer, 2008; Milyavsky et al., 2010; Zhang et al., 2011; Blanpain et al., 2011). Ceccaldi et al. demonstrated that BMF in FA is triggered by an exacerbated p53/p21 DNA damage response that impairs hematopoietic stem and progenitor cells (HSPC), leading to the progressive elimination of these cells in FA patients (Ceccaldi et al., 2012). Furthermore, hypersensitivity to cross-linking agents and thus the genomic instability can be restored to wild type (WT) levels in somatic FA cells when the NHEJ pathway is inhibited (Adamo et al., 2010; Pace et al., 2010). Whether NHEJ inhibition in FA-deficient cells would also restore the hematopoietic defects by reducing genomic instability and concomitant accumulation of DNA damage is unknown.

Although FA knockout mouse models have been established, they do not display spontaneous BMF and therefore do not fully mimic the hematopoietic condition seen in FA patients (Parmar et al., 2009). For this reason, a human disease model is more informative when investigating the mechanisms underlying the progressive BMF. Moreover it has been suggested that the hematopoietic defect in FA already starts *in utero* with a reduced HSPC pool during prenatal life, which is further challenged by additional age-related cellular stress and DNA damage resulting in HSPC exhaustion and BMF during childhood (Tulpule et al., 2010; Ceccaldi et al., 2012; Kamimae-Lanning et al., 2013). In this context, a human pluripotent stem cell model for FA would create an opportunity to interrogate the mechanism(s) underlying the decreased HSPC pool during development, and determine the role of aberrant NHEJ usage on hematopoiesis during the earliest stages of hematopoietic ontogeny, captured in the process of hematopoietic differentiation from pluripotent cells.

In 2009, Raya et al. found that somatic cells from FA patients could only be reprogrammed after correction of the genetic defect, suggesting an important role for the FA pathway in establishing pluripotency (Raya et al., 2009). However, Tulpule et al. subsequently created the first human-specific pluripotent FA stem cell model in hESC through knockdown (KD) of FA proteins using a lentiviral RNA interference (RNAi) approach (Tulpule et al., 2010). Recently it has been demonstrated that the reprogramming process itself triggers DNA damage and that efficient reprogramming requires key HR genes, including *Brca1*, *Brca2* (*Fancd1*) and *Rad51* (Gonzalez et al., 2013; Navarro et al., 2014). Given the close interplay of the FA and HR DNA repair pathways, it might not be surprising that difficulties are seen upon reprogramming FA-deficient cells. Nevertheless, several groups recently succeeded in reprogramming uncorrected FA patient cells, albeit with low efficiency (Muller et al., 2012; Yung et al., 2013; Liu et al., 2014). In addition, many of the established FA human induced pluripotent stem cell (hiPSC) lines could not be maintained in culture for more than a few passages (Yung et al., 2013). Together, these reports on FA hiPSC suggest an important role for the FA pathway not only in the establishment of pluripotency but also in the maintenance of pluripotent stem cells.

The aim of our study was to establish a human pluripotent disease model for FA through the creation of a *FANCA* knockout in hESC that would allow addressing the influence of loss of *FANCA* on hematopoietic development without interference of possible reprogramming-mediated mutations or the mutational load that somatic FA cells have collected during their life span, likely present in FA hiPSC. We demonstrate that *FANCA* knockout (*FANCA*−/−) hESC, in contrast to the previously established FA KD hESC model, display a severe growth disadvantage at the pluripotent stage, consistent with the notion that the FA pathway is vital for pluripotent stem cell proliferation.

Material and methods

hESC culture and maintenance

hESC line H9 (WA09) was purchased from WiCell Research Institute. H9 cells and all ZFN-targeted clones derived from it were expanded on inactivated mouse embryonic fibroblast (MEF) feeder layers in hESC medium (DMEM/F12 (Invitrogen) supplemented with 20% KnockOut Serum Replacement (Invitrogen), 1% non-essential amino acids (Invitrogen), 1 mM L-glutamine (Sigma-Aldrich), 0.1 mM β-mercaptoethanol (Sigma-Aldrich) and 4 ng/ml bFGF (Peprotech)). Feeder-free (FF) cultures for DNA sampling purposes were established by passaging the hESC onto Matrigel (Becton Dickinson)-coated plates in mTeSR I medium (Stemcell Technologies). Single cell dissociation to establish clonal cultures was performed with Trypsin 0.05% (Invitrogen) for MEF cultures or Accutase (Sigma) for FF cultures and cells were plated in medium containing 10 mM ROCK inhibitor (Sigma-Aldrich). Following the second targeting, cells were cultured at 37 °C in 5% CO_2 and 5% O_2.

FANCA targeting

A specific ZFN set for *FANCA* (Sigma-Aldrich) was generated targeting the first nucleotides of exon 2 (validation results in Fig. S1). A targeting vector carrying a selection cassette and homology arms flanking the double strand break was created so that its site-specific incorporation would disrupt the *FANCA* coding sequence (Fig. 1A). The different components for the *FANCA* targeting vector were cloned into the pCR2.1 plasmid (Life Technologies). The plasmids used for the first (Fig. S2) and second (Fig. S3) rounds of targeting carry Puromycin (Puro) and Hygromycin (Hygro) resistance cassettes respectively. Two million hESC were nucleofected with the targeting vector (11.5 μg for Puro and 12 μg for Hygro targeting) and 5 μl of ZFN mRNA using hESC Nucleofector solution 2 (Lonza), program A13 following the manufacturer's instructions. Cells were plated on inactivated DR4 MEF

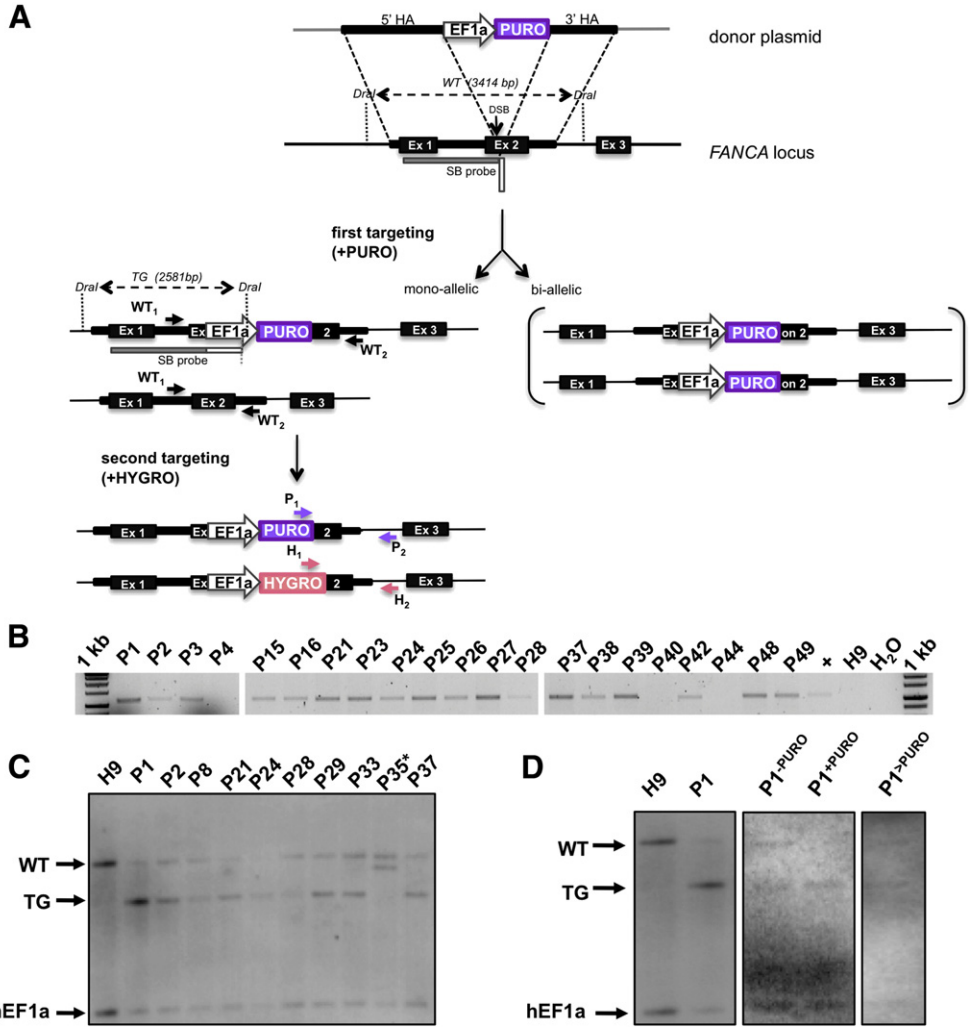

Figure 1 Schematic overview of ZFN-mediated *FANCA* targeting and demonstration of targeted integration in Puromycin-resistant clones. A) The *FANCA* locus and the expected modifications after each round of targeting are shown. Primers used to amplify the wild type allele (WT_1 + WT_2), the Puromycin (P_1 + P_2) and Hygromycin (H_1 + H_2) junctions by PCR are indicated. Thick black areas flanking the double strand break (DSB) depict homology arms (HA). Probe used for Southern blot (SB probe) is shown with a gray part annealing to the WT *FANCA* locus and a white part annealing to the EF1a promoter. Dashed vertical lines indicate DraI restriction sites for SB. B) Puromycin junction assay (primers P_1 + P_2) for a representative set of Puromycin-resistant clones with a positive control for the junction (P+) and untargeted hESC (H9) as a negative control. C) Southern blot (SB) results for representative set of Puromycin-resistant clones after DraI digest of genomic DNA. D) SB results after DraI digest shown for (left panel) clone 1 after initial selection but before Puromycin reselection (P1), (middle panel) clone 1 immediately after Puromycin reselection ($P1^{+PURO}$) and its unselected parallel culture at that time ($P1^{-PURO}$), (right panel) clone 1 some passages after Puromycin reselection ($P1^{>PURO}$). The probe anneals to both the transgenic EF1a promoter (TG) and the endogenous human EF1a promoter (hEF1a). hESC (H9) were taken as an untargeted reference for the wild type (WT) allele. Clones with random integration events are marked with *.

(GlobalStem) in media containing 10 mM ROCK inhibitor (Sigma-Aldrich). The Puro targeted hESC were selected with 300 ng/ml Puromycin (Sigma-Aldrich) and resistant colonies were individually picked and expanded after 7–13 days. After Hygro targeting, selection with up to 30 μg/ml of Hygromycin (Sigma-Aldrich) was performed. Surviving colonies were individually picked and expanded after 10 days. In the reselection process up to 500 ng/ml of Puromycin was used for Puro targeted clones and concentrations up to 50 μg/ml of Hygromycin in the case of Hygromycin reselection.

PCR genotyping

Genotyping PCRs were performed according to standard procedures using primers listed in Table S4. A schematic representation of the primer pairs can be found in Fig. 1A. For the Puromycin and Hygromycin junction assays a forward primer annealing to the selection cassette and a reverse primer in the *FANCA* locus outside the homology arms (HA) were combined. The correct amplification of the junctions was confirmed through sequencing both in controls and

samples. Positive controls used for the junction assays are listed in Table S5. Primers flanking the double strand break (DSB) were used for the WT allele amplification assay and correct amplification was confirmed through sequencing. To assess random integration by PCR two sets of primers were designed along the backbone of the plasmid used during ZFN-mediated targeting.

Proliferation kinetics

The growth delay of clones cultured on MEF and on Matrigel (FF) was visualized by plotting the subsequent passages (y-axis) against a cumulative growth delay factor (x-axis), which was calculated as follows: time to reach confluence (time between subsequent passages in days) divided by expansion factor: "time to confluence/expansion factor". This means that the longer it takes for a culture to become confluent (increase in numerator) or the less it can be expanded (decrease in denominator), the bigger the increase on the x-axis. This will result in a flatter slope for slow growing cultures and a steeper slope for fast growing cultures. The values used to calculate the cumulative growth delay for each cell line can be found in Table S6 (MEF) and Table S7 (FF).

Southern blot analysis

Genomic DNA was isolated using the QiaAmp DNA mini kit (Qiagen). Southern blots were performed using the DIG High Prime DNA Labeling and Detection starter kit II (Roche) according to the manufacturer's instructions. The primer set used for the generation of the Southern blot probe can be found in Table S4. A schematic representation of the probe and the fragment sizes after DraI (Fermentas) digestion can be found in Fig. 1A.

aCGH

Genomic DNA was isolated using the QiaAmp DNA mini kit (Qiagen). Samples were hybridized against commercially available female control DNA (Kreatech) and subjected to a whole genome analysis using 180 k Cytosure ISCA v2 arrays (Oxford Gene Technologies). Array data were extracted using Feature Extraction software v10.7 and visualized using CytoSure Interpret Software V4.5.3. Copy number altered regions were detected using statistics provided by the CytoSure Interpret Software V4.5.3, considering a minimum number of five consecutive probes.

Western blot analysis

Western blot analysis was performed using a rabbit polyclonal antibody for FANCA (1:2000; Abcam) and a mouse monoclonal antibody for GAPDH (1:5000; Santa Cruz Biotechnology) followed by horseradish peroxidase-conjugated swine anti-rabbit secondary antibody (1:3000; Dako) and goat anti-mouse secondary antibody (1:3000; Dako) respectively.

QuantiGene® FlowRNA assay

Probes against Puromycin N-acetyl-transferase and hygromycin B phosphotransferase mRNA transcripts were designed by Affymetrix. The QuantiGene® FlowRNA assay (Affymetrix) was conducted according to the manufacturer's instructions. Data was analyzed by FlowJo software.

Results

Growth advantage for *FANCA*+/− hESC over *FANCA*−/− hESC

To create a human pluripotent stem cell model for FA, we aimed at knocking out *FANCA* in hESC through insertion of a Puromycin resistance (Puro) cassette in exon 2, thereby disrupting the *FANCA* coding sequence. As FA is a recessive disease, bi-allelic targeting is required to establish the appropriate model. After nucleofection of hESC (H9) with a *FANCA*-specific ZFN pair and a donor plasmid harboring a Puro cassette flanked by homology arms (HA) (Fig. 1A), recombinant clones were selected with 300 ng/ml Puromycin. Resistant colonies were picked after 7–13 days of selection and site-specific integration of the Puro cassette could be demonstrated in 37 out of 50 clones through amplification of the cassette junction by PCR (Fig. 1B). Southern blot (SB) data confirmed the targeted integration of the Puro cassette but as the WT allele could still be detected in all clones, no bi-allelic targeting events could be identified (Fig. 1C). For one clone (clone P1), SB suggested a higher abundance of transgenic than WT alleles (Fig. 1C). As hESC were split as clumps rather than through single cell dissociation, we hypothesized that this clone might represent a mixture of mono-allelically (*FANCA*+/−) and bi-allelically (*FANCA*−/−) targeted cells both withstanding the applied selection pressure. Disappearance of the band corresponding to the WT allele upon reselection with 500 ng/ml Puromycin confirmed this hypothesis (Fig. 1D). This coincided with the observation that some colonies in the culture disappeared upon reselection whereas others seemed not to be affected by this higher concentration. However, when the same clone was assessed by SB a few passages after Puromycin reselection, the WT allele was again detected (Fig. 1D), suggesting a selective growth advantage of *FANCA*+/− cells, which can escape or withstand selection pressure, over *FANCA*−/− cells.

FANCA −/− hESC display a severe growth disadvantage resulting in growth arrest

As we were unable to maintain bi-allelically targeted hESC as a pure population of *FANCA*−/− cells, we adopted an alternative targeting approach wherein we nucleofected mono-allelically targeted hESC (*FANCA*+/−) with a second selection cassette (Fig. 1A). First, an additional round of Puromycin selection was conducted on a clone previously confirmed to carry a unique insertion of the Puro cassette in *FANCA* (clone P21) to eliminate possible remnants of untargeted cells. Next, a Hygromycin resistance (Hygro) cassette was inserted into the untargeted allele via a second round of ZFN-mediated HR. We identified several clones

carrying both a Hygro and a Puro cassette in the *FANCA* locus as judged by the amplification of the respective junctions by PCR (Figs. 2A,B). Further confirmation of bi-allelic targeting was seen in the inability to amplify the WT allele in some of these (Fig. 2C). Clones fitting all three criteria of bi-allelic targeting (clones PH4, PH16 and PH18) were chosen for further expansion, as these were considered *FANCA*−/− hESC.

Though undetectable in the first passage after ZFN targeting, the WT *FANCA* allele could again be amplified in nearly all clones the next passage both in cultures on inactivated mouse embryonic fibroblasts (MEF) as well as in feeder-free (FF) cultures (Figs. 2D, E). The different amplicons were sequenced to verify that they indeed represented the expected cassette junctions or WT allele. To further purify *FANCA*−/− cells, Hygromycin selection was reinitiated. The three bi-allellically targeted clones cultured on MEF showed a profound growth delay and underwent growth arrest one passage (19–22 days) after reinitiation of Hygromycin selection (Fig. 3A). Following splitting, only a few colonies attached. The colonies that attached displayed the characteristic hESC appearance without any signs of differentiation but showed only a minimal increase in size and after some time remained as such without any visible growth. Clones maintained feeder-free however, though clearly affected, did not all display the same rate of growth arrest as on MEF (Fig. 3B). The most severe growth delay was seen in clone PH16 where, in contrast to other clones, the WT allele did not reappear immediately the next passage. Whereas culture of untargeted hESC on Matrigel requires colonies to be split about every 5 days, clone PH16 did not reach confluency even after 14 days in the absence of selection. Clone PH18 on the other hand, clearly affected by Hygromycin selection as the time between subsequent passages increased to roughly two-fold the regular 5-day interval, could be kept in culture for an extended number of passages. DNA taken at subsequent passages under Hygromycin reselection continuously showed amplification of the WT allele in addition to both cassette junctions (Figs. 3C,D,E). The presence of WT *FANCA* in spite of clear demonstration of bi-allelic targeting in PH18 was further substantiated by Western blot data demonstrating FANCA protein expression (Fig. 3F). Attempts to establish clonal cultures from this clone and others through single cell dissociation were not successful as few cells grew out to become colonies and these quickly displayed growth arrest.

Demonstration of bi-allelic targeting at the single cell level

To unequivocally demonstrate that *FANCA* knockout cells are present within this culture initially confirmed to be bi-allelically targeted based on the amplification of both Puro and Hygro cassette junctions and the absence of the WT allele, we made use of the QuantiGene® FlowRNA assay. Using probes against Puromycin N-acetyl-transferase and Hygromycin B phosphotransferase mRNA transcripts we analyzed whether these selection cassette transcripts were present together at the single cell level. The FlowRNA assay clearly demonstrates that clone PH18 harbors a population of cells positive for both the Puro and Hygro cassettes (Fig. 4A). As we also verified the absence of random integrations in this clone both by SB and PCR (Figs. 4B, C), we can safely conclude that this population represents a *FANCA* knockout hESC population with a Puro cassette disrupting one allele of *FANCA* and a Hygro cassette disrupting the other.

Heterogeneity in FANCA−/− cultures

As FA is associated with genomic instability and genetic rearrangements are recurrently found in iPSC generated from FA-deficient cells (Muller et al., 2012; Yung et al., 2013), we investigated whether rearrangements in the genome of these bi-allelically targeted clones could possibly explain the

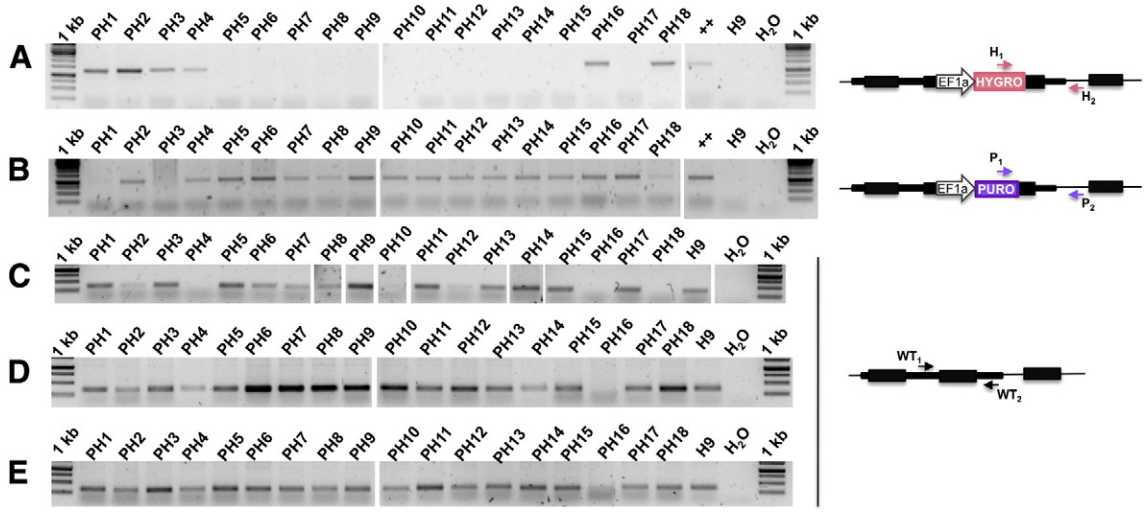

Figure 2 PCR genotyping for Hygromycin-resistant clones. A–E) PCR genotyping results during the first two passages of Hygromycin-resistant clones. A) Hygromycin junction assay with a positive control for the junction (H+) and untargeted hESC (H9) as a negative control. B) Puromycin junction assay with a positive control for the junction (P+) and untargeted hESC (H9) as a negative control. C–E) Wild type allele amplification assay at the first passage after picking Hygromycin-resistant colonies (C) or after one additional passage on MEF (D) or in FF conditions (E). H9 are included as a positive control for the WT locus.

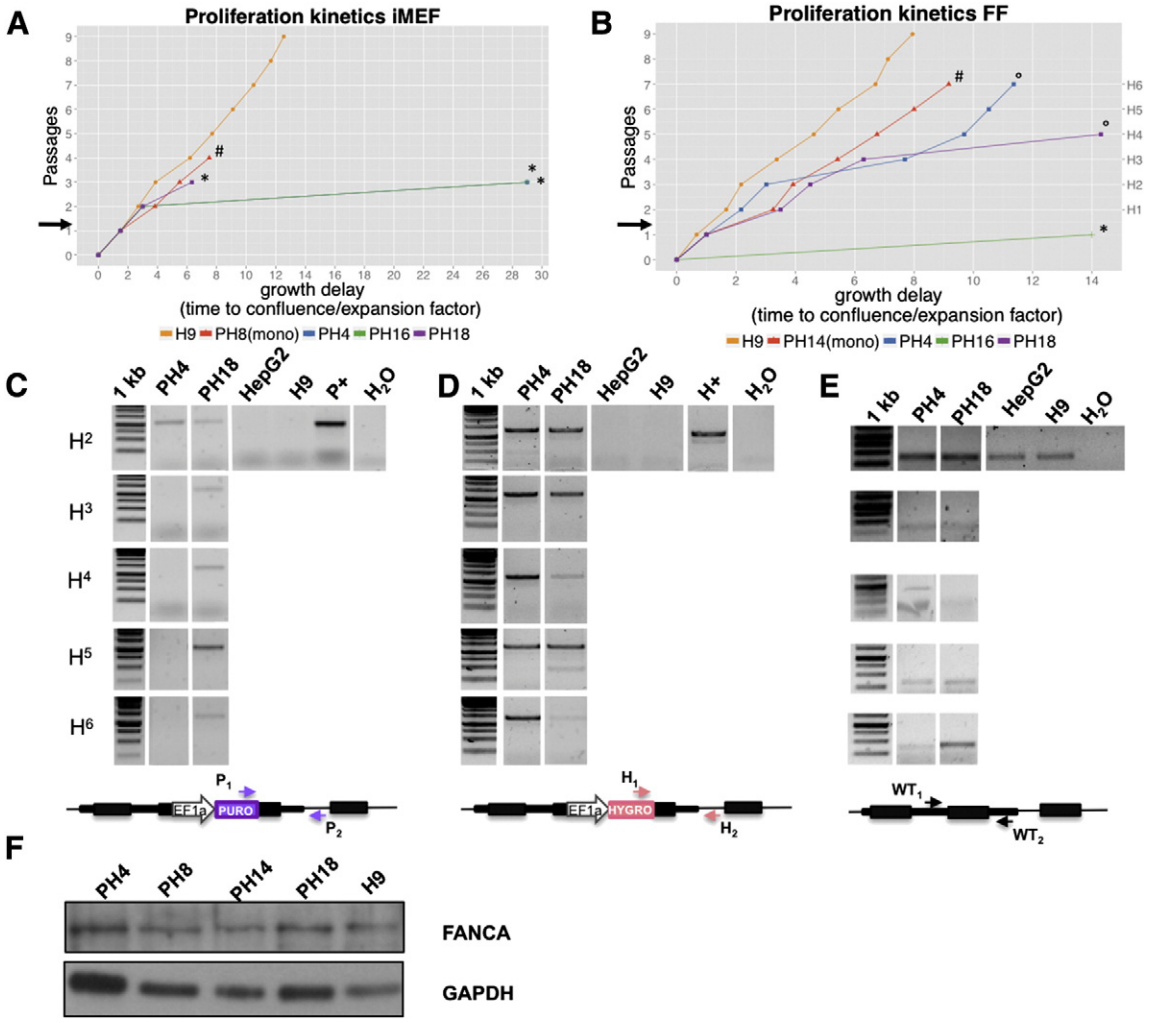

Figure 3 Bi-allelically targeted clones show a severe growth disadvantage and a persistent presence of WT *FANCA* in those cultures that can be maintained in culture. A) Proliferation kinetics of cultures on MEF. Values on the x-axis are representative for the growth delay a certain cell line displays. These values are calculated as time to reach confluence (time between subsequent passages in days) divided by expansion factor: "time to confluence/expansion factor". This means that the longer it takes for a culture to be confluent (increase in numerator) or the less it can be expanded (increase in denominator), the bigger the increase on the x-axis. This will result in a flatter slope for slow growing cultures and a steeper slope for fast growing cultures. The arrow indicates the start of Hygromycin reselection. Untargeted H9 (H9) are included as a reference (unselected) and a mono-allelically Hygro targeted cell line (PH8(mono)) cultured in parallel under the same Hygromycin selection regimen is included as a control. * indicates when maintenance of the culture became impossible due to growth arrest. # represents the point at which a confluent culture was frozen. B) Proliferation kinetics of FF cultures. Passages under Hygromycin reselection are labeled as H^1–H^6 on the right axis. The arrow indicates the start of Hygromycin reselection. Untargeted H9 (H9) are included as a reference (unselected) and a mono-allelically Hygro targeted cell line (PH14(mono)) cultured in parallel under the same Hygromycin selection regimen is included as a control. * indicates when maintenance of the culture became impossible due to growth arrest. # represents the point at which a confluent culture was frozen. ° indicates the point at which cultures were discontinued due to persistent heterogeneity or after the confirmation of loss of the *FANCA*−/− cells. C) Puromycin junction assay with a positive control for the junction (P+) and untargeted HepG2 and H9 as negative controls. D) Hygromycin junction assay with a positive control for the junction (H+) and untargeted HepG2 and H9 as negative controls. E) Wild type allele amplification assay with untargeted HepG2 and H9 included as positive controls for the WT locus. F) Western blot showing FANCA expression in Hygromycin-resistant clones with untargeted H9 as a reference.

genotyping results, where three different versions of the *FANCA* locus could be identified. An array comparative genomic hybridization (aCGH) screen was performed on clones PH4 and PH18 (Fig. 5), which did not reveal significant copy number variations compared to the untargeted hESC line or clone P21 used for the second round of targeting with a Hygro cassette. For clone PH18 however, a duplication of 6.6 Mb on the short arm of chromosome 5 (5p14.1p13.2(28,340,612–35,004,191) × 3) was detected shortly after targeting that was not present in clone P21 from which the clone was derived. The duplication could no longer be detected in a subsequent sample of clone PH18 following a few passages. This suggests that this duplication arose in a subpopulation of cells that then disappeared from the culture over the next passages.

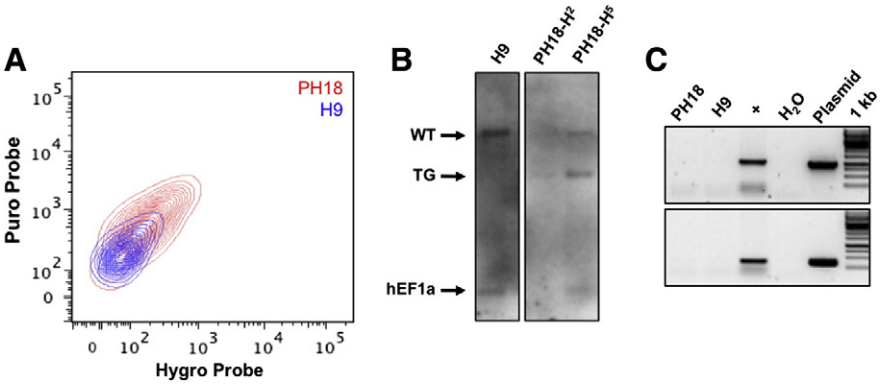

Figure 4 Demonstration of bi-allelic targeting at the single cell level. A) Flow RNA plot showing Puromycin N-acetyl-transferase (Puro probe) and Hygromycin B phosphotransferase (Hygro probe) expression for clone PH18 (red) compared to untargeted H9 (blue). B) Southern blot after DraI digest for clone PH18 after 2 (H^2) and 5 (H^5) passages under Hygromycin reselection demonstrating absence of random integrations. C) PCR results demonstrating absence of random integrations. Untargeted H9 were included as negative control. Positive controls are HEK293 harboring randomly integrated pieces of the plasmid used for targeting (+) and the targeting plasmid itself (plasmid). Upper and lower panels represent primers spanning the backbones 3′ and 5′ from the selection cassette respectively.

More evidence for selective outgrowth of subpopulations of cells were found in the behavior of clone PH4. PCR data showed that for clone PH4 the Puro junction could no longer be amplified at passage 3 during Hygromycin reselection (H^3) whereas the passage before (H^2) (Fig. 3C) it was still present. This was confirmed by the simultaneous loss of Puromycin resistance; hence again creating a mono-allelically targeted cell population. This is consistent with the hypothesis that the culture remains mixed, and that the *FANCA*−/− subpopulation disappears due to its inherent growth disadvantage while others, not bi-allelically targeted, take over the culture. Further corroborating this hypothesis is the fact that the H^2 culture required 14 days to reach sufficient confluence to be split into H^3 (Fig. 3B). From H^3 onwards, the growth rate of the now mono-allelically targeted cells was restored to levels similar to those of untargeted H9.

Discussion

Fanconi anemia is an intriguing yet devastating condition at the intersection of DNA repair and hematopoietic dysfunction. Whereas the functions of FA proteins in DNA repair are well documented (Moldovan and D'Andrea, 2009; de Winter and Joenje, 2009), the mechanism underlying the characteristic BMF is less well understood as many model systems, including FA knockout mice, fail to recapitulate the hematopoietic phenotype in all its aspects (Parmar et al., 2009). Recently however, clues on how these two features are linked came from the demonstration that an exacerbated p53/p21 DNA damage response impairs HSPC causing progressive elimination of these cells in FA patients, ultimately resulting in BMF (Ceccaldi et al., 2012). Compared with normal fetal liver samples, p21 levels in the liver from FA fetuses were significantly higher, consistent with the onset of FA-induced loss of HSPC during prenatal life. To identify the earliest effects of FA deficiency on hematopoietic development, we aimed at creating a human pluripotent FA stem cell model. We generated a *FANCA* knockout in hESC via ZFN-mediated HR, disrupting both alleles of *FANCA*. Such *FANCA* knockout hESC, however, displayed a severe growth disadvantage, which paves the way for non-FA-deficient cells, be it mono-allelically targeted or untargeted cells, to take over the culture as they have a growth advantage over the FA-deficient cells. When *FANCA*−/− hESC were purified from these contaminating cells, either through selection or single cell cloning, they rapidly underwent growth arrest and such cultures could not be maintained, making them not suitable as a FA disease model.

Interfering with DNA repair at the pluripotent stage, tightly regulated not to propagate mutations to its progeny (Fortini et al., 2013; Rocha et al., 2013), is not without risks. However, no problems in the maintenance of pluripotent cells were reported after knocking down FA proteins in hESC (Tulpule et al., 2010). Loss of p53 and ATM in hESC, to model two major genetic instability syndromes, also did not affect hESC proliferation (Song et al., 2010). Nevertheless, we here demonstrate that whereas mono-allelically targeted cells have unaltered proliferation potential compared to untargeted hESC, disruption of the second *FANCA* allele causes a severe growth disadvantage.

Initially it was postulated that a functional FA pathway is a prerequisite for cells to be reprogrammed to the pluripotent stage as reprogramming could only be achieved in FA patient cells after correction of the FA defect (Raya et al., 2009). More recently however, several groups demonstrated that FA cells are resistant but not refractory to reprogramming as they succeeded in generating FA iPSC, albeit at a greatly reduced efficiency (Muller et al., 2012; Yung et al., 2013; Navarro et al., 2014; Liu et al., 2014). Although Yung et al. succeeded in reprogramming FA patient cells under normoxic conditions, Muller et al. described a disease-associated advantage for reprogramming FA cells under hypoxia and therefore used hypoxic conditions to generate FA hiPSC (Muller et al., 2012; Yung et al., 2013). In contrast to these reports and in agreement with an exacerbated p53 stress response in FA cells (Ceccaldi et al., 2012) and the rate-limiting effect of p53 on reprogramming (Marion et al., 2009; Hong et al., 2009; Utikal et al., 2009), Liu et al. could only generate FA hiPSC when p53 shRNA was added to the reprogramming cocktail (Liu et al., 2014). When p53

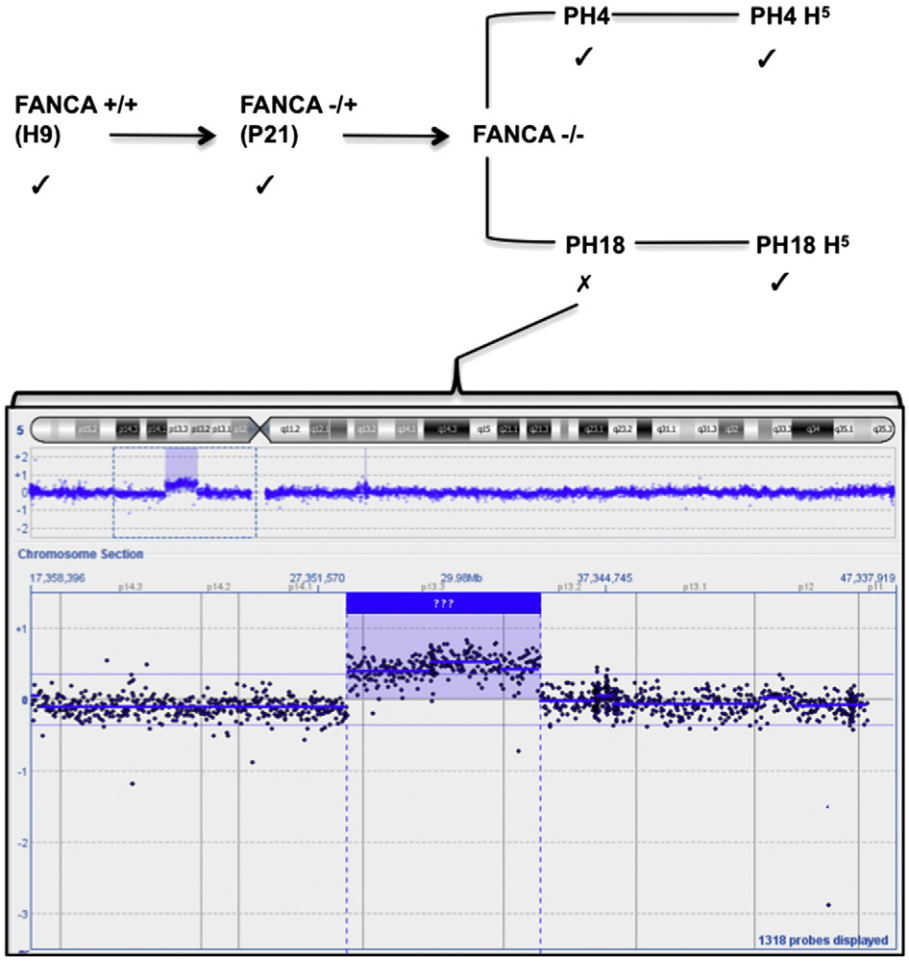

Figure 5 aCGH data showing a duplication of 6.6 Mb at the short arm of chromosome 5 in clone PH18 shortly after targeting. Clones PH4 and PH18 were analyzed by aCGH shortly after targeting and following 5 passages under Hygromycin reselection (H^5). Untargeted H9 cells and clone P21 from which clones PH4 and PH18 are derived were included in the screen as references. Log2 ratios are depicted on the vertical axis.

shRNA was omitted, reprogramming barriers could not be overcome despite the presence of epigenetic remodeler sodium butyrate and hypoxic conditions. The integration-free FA hiPSC generated in this study displayed slower kinetics as they appeared only after 40 (instead of 22) days of reprogramming. Moreover, a threefold reduction in the amount of colonies present after seeding similar numbers of cells was observed for FA hiPSC compared to control hiPSC (Liu et al., 2014). Besides this decrease in clonogenicity described by Liu et al., also the proliferation and/or maintenance of previously generated FA hiPSC lines seemed to be compromised. Whereas Muller et al. mentioned slightly delayed growth kinetics in FA hiPSC, Yung et al. reported that most of the FA hiPSC lines established in their study could not be maintained in culture for more than a few passages (Muller et al., 2012; Yung et al., 2013). The only two lines that could be maintained had a very abnormal karyotype, which leaves room to speculate that genetic events possibly compensating for the absence of the FA pathway enabled successful reprogramming and maintenance (Yung et al., 2013). This would be consistent with the observation that corrected FA iPSC fail to silence the transgenic *FANCA* copy after reprogramming, suggesting a selective pressure for continued correction of the FA pathway and that knockdown of the *FANCA* transgene resulted in loss of hiPSC proliferation (Raya et al., 2009; Muller et al., 2012). Combined with these data, our findings convincingly support the relevance of a functional FA pathway for the maintenance of pluripotent stem cells.

While others and we find that maintenance of pluripotent stem cells is compromised in case of a defective FA pathway, total absence of FANCA protein in humans does not reduce embryonic viability (Castella et al., 2011). Most likely this discrepancy can be contributed to the fact that hESC and hiPSC are the *in vitro* equivalents of pluripotent cells found in the blastocyst, artificially maintained in the undifferentiated state through tailor-made culture conditions that continuously stimulate the cells to divide symmetrically. These *in vitro* stimuli expose the cells to high levels of replicative stress that might not be present *in vivo*, or only for a short period of time. In addition hESC and hiPSC are inevitably exposed to oxidative stress during culture and when handling the cells. Considering the sensitivity of FA-deficient cells to oxidative and replicative stress (Joenje et al., 1981; Schindler and Hoehn, 1988; Ceccaldi et al., 2012), these elevated levels in culture *in vitro* compared to *in vivo* likely account for an accumulation of DNA damage at a stage tightly controlled not to propagate mutations to the progeny. This

might well be the underlying cause of the accelerated replicative crisis observed in *FANCA* knockout hESC and FA hiPSC.

In this study we were also confronted with heterogeneous cultures of mono-allelically and bi-allelically targeted cells both withstanding the applied selection pressure. Similar mixtures have been reported after ZFN targeting (Yao et al., 2012) and are a direct consequence of the fact that hESC are generally passaged as clumps rather than through single cell dissociation. Immediately after targeting, the cells are plated as single cells, which then grow into resistant colonies during the selection process. When selection is complete, judged by the elimination of untargeted cells in a control well exposed to the same concentration of the antibiotic, resistant colonies are manually cut in smaller pieces to establish a subculture. The resulting culture is not necessarily clonal in nature, as we cannot exclude the presence of different cell clones in one resistant colony. In fact, data obtained shortly after targeting suggests the co-existence of some incompletely targeted cells amongst the bulk of bi-allelically targeted hESC as the WT band that could not be detected by PCR in the first passage after targeting could again be amplified one passage later in most clones. This demonstrates that non-FA-deficient cells, even when representing a negligible percentage of the total population, quickly out-proliferate *FANCA* knockout cells due to the inherent growth disadvantage of the latter. This observation is akin to somatic mosaicism which confers a selective growth advantage over FA-deficient cells onto their gene corrected counterparts (Waisfisz et al., 1999; Gregory et al., 2001; Gross et al., 2002). Moreover our data suggest that even though antibiotic concentrations were used that were carefully titrated to result in complete elimination of unmodified hESC, still some untargeted cells managed to persist and give rise to heterogeneous cultures. Attempts to establish clonal cultures through single cell dissociation to circumvent this issue were not successful as the few colonies that grew out rapidly displayed growth arrest.

Given the severely compromised proliferation upon disruption of the second *FANCA* allele, we have considered combining the knockout strategy with an inducible overexpression of *FANCA*, which would allow bi-allelic targeting in the presence of a functional FA pathway. Even though this could facilitate the initial characterization of the bi-allelic targeting, at the point where we would induce the knockout by removing the transgenic *FANCA* expression, similar complications as discussed above would most likely arise. Irrespective of the method (Cre–LoxP, FRT–Flipase, doxycycline inducible systems), it remains challenging to completely eliminate the expression of the transgenic FANCA in all cells of the culture. As our data show that even a negligible amount of non-FA-deficient cells can quickly take over resulting in a heterogeneous culture and that rapid growth arrest occurs when we try to circumvent such heterogeneity issues by generating clonal knockout cell lines, we believe that considerable technical challenges will prevent us from obtaining a pure FANCA−/− population for further functional testing, even with a conditional approach.

Conclusion

The inherent growth defect of *FANCA* knockout hESC reported in this study hampers the establishment of a human pluripotent FA disease model and therefore our question whether disabling error-prone DNA repair in a FA context would restore hematopoiesis, as it does for the genomic instability in somatic FA cells, remains unanswered. The creation of a *FANCA* knockout in hESC however did allow us to address the consequences of a complete loss of *FANCA* at the pluripotent stage in an unbiased way as the cells established in this study did not carry any mutational load associated with reprogramming in a DNA repair-deficient context. We show that disabling the FA pathway in hESC by disrupting both copies of *FANCA* (*FANCA*−/−) leads to a severe growth disadvantage, ultimately resulting in growth arrest. As such, *FANCA* knockout hESC surface additional problems compared to a FA KD hESC model, possibly reflecting a difference between the complete absence of a functional FA pathway and presence of some residual FA proteins, albeit at very low amounts. It cannot be excluded however that other variables such as the culture system and in vitro stress levels are also in part responsible for the extent to which a growth deficit becomes apparent as a recently generated *FANCA* knockout hESC model displayed milder growth deficits at the pluripotent stage than what is reported here (Liu et al., 2014). Nevertheless, the demonstration that proliferation is compromised in FA-deficient pluripotent stem cells is a consistent observation in agreement with recent reports on FA hiPSC and emphasizes the importance of a functional FA pathway at the pluripotent stem cell stage.

Acknowledgments

The authors acknowledge Rob Van Rossom and Thomas Vanwelden for technical assistance.

KV and QC were funded by IWT (SB-091228 and SB-093228; SB-71255 and SB-73255); LO by Gobierno de Aragon (FMI048/08), Instituto Aragonés de Ciencias de la Salud (BPAMER3/08/04) and IWT (OZM-090838). SK was funded by FWO (PDO/10 and KAN2014). KU Leuven (SCIL PF/10/019, OT/09/053, EJJ-C6086-2012-194, EJJ-C2584-G.0851.11), BELSPO-IUAP-DEVREPAIR (EJJ-C4851-P7/07-P), FWO G.0452.06 and FWO Odysseus award (G.0667.07) were granted to CMV.

Authorship contributions

KV designed and performed the research, analyzed and interpreted the results and wrote the manuscript. QC designed the research and interpreted results. NN and SS performed the research and analyzed the results. SK analyzed the data, interpreted the results and edited the manuscript. JRV designed the aCGH experiments, interpreted the results and edited the manuscript. LO and CMV designed the research, interpreted the results and edited the manuscript.

Appendix A. Supplementary data

Supplementary data to this article can be found online at http://dx.doi.org/10.1016/j.scr.2014.07.005.

References

Adamo, A., Collis, S.J., Adelman, C.A., Silva, N., Horejsi, Z., Ward, J.D., Martinez-Perez, E., Boulton, S.J., La Volpe, A., 2010. Preventing nonhomologous end joining suppresses DNA repair defects of Fanconi

anemia. Mol. Cell 39 (1), 25–35. http://dx.doi.org/10.1016/j.molcel.2010.06.026 (S1097-2765(10)00493-4 [pii]).

Auerbach, A.D., 2009. Fanconi anemia and its diagnosis. Mutat. Res. 668 (1–2), 4–10. http://dx.doi.org/10.1016/j.mrfmmm.2009.01.013 (S0027-5107(09)00053-0 [pii]).

Auerbach, A.D., Rogatko, A., Schroeder-Kurth, T.M., 1989. International Fanconi Anemia Registry: relation of clinical symptoms to diepoxybutane sensitivity. Blood 73 (2), 391–396.

Blanpain, C., Mohrin, M., Sotiropoulou, P.A., Passegue, E., 2011. DNA-damage response in tissue-specific and cancer stem cells. Cell Stem Cell 8 (1), 16–29. http://dx.doi.org/10.1016/j.stem.2010.12.012 (S1934-5909(10)00707-1 [pii]).

Castella, M., Pujol, R., Callen, E., Trujillo, J.P., Casado, J.A., Gille, H., Lach, F.P., Auerbach, A.D., Schindler, D., Benitez, J., Porto, B., Ferro, T., Munoz, A., Sevilla, J., Madero, L., Cela, E., Belendez, C., de Heredia, C.D., Olive, T., de Toledo, J.S., Badell, I., Torrent, M., Estella, J., Dasi, A., Rodriguez-Villa, A., Gomez, P., Barbot, J., Tapia, M., Molines, A., Figuera, A., Bueren, J.A., Surralles, J., 2011. Origin, functional role, and clinical impact of Fanconi anemia FANCA mutations. Blood 117 (14), 3759–3769. http://dx.doi.org/10.1182/blood-2010-08-299917 (blood-2010-08-299917 [pii]).

Ceccaldi, R., Parmar, K., Mouly, E., Delord, M., Kim, J.M., Regairaz, M., Pla, M., Vasquez, N., Zhang, Q.S., Pondarre, C., Peffault de Latour, R., Gluckman, E., Cavazzana-Calvo, M., Leblanc, T., Larghero, J., Grompe, M., Socie, G., D'Andrea, A.D., Soulier, J., 2012. Bone marrow failure in Fanconi anemia is triggered by an exacerbated p53/p21 DNA damage response that impairs hematopoietic stem and progenitor cells. Cell Stem Cell 11 (1), 36–49. http://dx.doi.org/10.1016/j.stem.2012.05.013 (S1934-5909(12)00247-0 [pii]).

de Winter, J.P., Joenje, H., 2009. The genetic and molecular basis of Fanconi anemia. Mutat. Res. 668 (1–2), 11–19. http://dx.doi.org/10.1016/j.mrfmmm.2008.11.004 (S0027-5107(08)00282-0 [pii]).

Fortini, P., Ferretti, C., Dogliotti, E., 2013. The response to DNA damage during differentiation: pathways and consequences. Mutat. Res. 743–744, 160–168. http://dx.doi.org/10.1016/j.mrfmmm.2013.03.004 (S0027-5107(13)00022-5 [pii]).

Garaycoechea, J.I., Patel, K.J., 2014. Why does the bone marrow fail in Fanconi anemia? Blood 123 (1), 26–34. http://dx.doi.org/10.1182/blood-2013-09-427740 (blood-2013-09-427740 [pii]).

Gonzalez, F., Georgieva, D., Vanoli, F., Shi, Z.D., Stadtfeld, M., Ludwig, T., Jasin, M., Huangfu, D., 2013. Homologous recombination DNA repair genes play a critical role in reprogramming to a pluripotent state. Cell Rep. 3 (3), 651–660. http://dx.doi.org/10.1016/j.celrep.2013.02.005 (S2211-1247(13)00064-8 [pii]).

Gregory Jr., J.J., Wagner, J.E., Verlander, P.C., Levran, O., Batish, S.D., Eide, C.R., Steffenhagen, A., Hirsch, B., Auerbach, A.D., 2001. Somatic mosaicism in Fanconi anemia: evidence of genotypic reversion in lymphohematopoietic stem cells. Proc. Natl. Acad. Sci. U. S. A. 98 (5), 2532–2537. http://dx.doi.org/10.1073/pnas.051609898 (051609898 [pii]).

Gross, M., Hanenberg, H., Lobitz, S., Friedl, R., Herterich, S., Dietrich, R., Gruhn, B., Schindler, D., Hoehn, H., 2002. Reverse mosaicism in Fanconi anemia: natural gene therapy via molecular self-correction. Cytogenet. Genome Res. 98 (2–3), 126–135 (doi: 6980569805 [pii]).

Hong, H., Takahashi, K., Ichisaka, T., Aoi, T., Kanagawa, O., Nakagawa, M., Okita, K., Yamanaka, S., 2009. Suppression of induced pluripotent stem cell generation by the p53–p21 pathway. Nature 460 (7259), 1132–1135. http://dx.doi.org/10.1038/nature08235 (nature08235 [pii]).

Ishida, R., Buchwald, M., 1982. Susceptibility of Fanconi's anemia lymphoblasts to DNA-cross-linking and alkylating agents. Cancer Res. 42 (10), 4000–4006.

Joenje, H., Arwert, F., Eriksson, A.W., de Koning, H., Oostra, A.B., 1981. Oxygen-dependence of chromosomal aberrations in Fanconi's anaemia. Nature 290 (5802), 142–143.

Kamimae-Lanning, A.N., Goloviznina, N.A., Kurre, P., 2013. Fetal origins of hematopoietic failure in a murine model of Fanconi anemia. Blood 121 (11), 2008–2012. http://dx.doi.org/10.1182/blood-2012-06-439679 (blood-2012-06-439679 [pii]).

Kee, Y., D'Andrea, A.D., 2010. Expanded roles of the Fanconi anemia pathway in preserving genomic stability. Genes Dev. 24 (16), 1680–1694. http://dx.doi.org/10.1101/gad.1955310 (24/16/1680 [pii]).

Kutler, D.I., Singh, B., Satagopan, J., Batish, S.D., Berwick, M., Giampietro, P.F., Hanenberg, H., Auerbach, A.D., 2003. A 20-year perspective on the International Fanconi Anemia Registry (IFAR). Blood 101 (4), 1249–1256. http://dx.doi.org/10.1182/blood-2002-07-2170 (2002-07-2170 [pii]).

Liu, G.H., Suzuki, K., Li, M., Qu, J., Montserrat, N., Tarantino, C., Gu, Y., Yi, F., Xu, X., Zhang, W., Ruiz, S., Plongthongkum, N., Zhang, K., Masuda, S., Nivet, E., Tsunekawa, Y., Soligalla, R.D., Goebl, A., Aizawa, E., Kim, N.Y., Kim, J., Dubova, I., Li, Y., Ren, R., Benner, C., Del Sol, A., Bueren, J., Trujillo, J.P., Surralles, J., Cappelli, E., Dufour, C., Esteban, C.R., Izpisua Belmonte, J.C., 2014. Modelling Fanconi anemia pathogenesis and therapeutics using integration-free patient-derived iPSCs. Nat. Commun. 5, 4330. http://dx.doi.org/10.1038/ncomms5330 (ncomms5330 [pii]).

Look, A.T., 1997. Oncogenic transcription factors in the human acute leukemias. Science 278 (5340), 1059–1064.

Marion, R.M., Strati, K., Li, H., Murga, M., Blanco, R., Ortega, S., Fernandez-Capetillo, O., Serrano, M., Blasco, M.A., 2009. A p53-mediated DNA damage response limits reprogramming to ensure iPS cell genomic integrity. Nature 460 (7259), 1149–1153. http://dx.doi.org/10.1038/nature08287 (nature08287 [pii]).

Milyavsky, M., Gan, O.I., Trottier, M., Komosa, M., Tabach, O., Notta, F., Lechman, E., Hermans, K.G., Eppert, K., Konovalova, Z., Ornatsky, O., Domany, E., Meyn, M.S., Dick, J.E., 2010. A distinctive DNA damage response in human hematopoietic stem cells reveals an apoptosis-independent role for p53 in self-renewal. Cell Stem Cell 7 (2), 186–197. http://dx.doi.org/10.1016/j.stem.2010.05.016 (S1934-5909(10)00226-2 [pii]).

Moldovan, G.L., D'Andrea, A.D., 2009. How the Fanconi anemia pathway guards the genome. Annu. Rev. Genet. 43, 223–249. http://dx.doi.org/10.1146/annurev-genet-102108-134222.

Muller, L.U., Milsom, M.D., Harris, C.E., Vyas, R., Brumme, K.M., Parmar, K., Moreau, L.A., Schambach, A., Park, I.H., London, W.B., Strait, K., Schlaeger, T., Devine, A.L., Grassman, E., D'Andrea, A., Daley, G.Q., Williams, D.A., 2012. Overcoming reprogramming resistance of Fanconi anemia cells. Blood 119 (23), 5449–5457. http://dx.doi.org/10.1182/blood-2012-02-408674 (blood-2012-02-408674 [pii]).

Navarro, S., Moleiro, V., Molina-Estevez, F.J., Lozano, M.L., Chinchon, R., Almarza, E., Quintana-Bustamante, O., Mostoslavsky, G., Maetzig, T., Galla, M., Heinz, N., Schiedlmeier, B., Torres, Y., Modlich, U., Samper, E., Rio, P., Segovia, J.C., Raya, A., Guenechea, G., Izpisua-Belmonte, J.C., Bueren, J.A., 2014. Generation of iPSCs from genetically corrected Brca2 hypomorphic cells: implications in cell reprogramming and stem cell therapy. Stem Cells 32 (2), 436–446. http://dx.doi.org/10.1002/stem.1586.

Niedernhofer, L.J., 2008. DNA repair is crucial for maintaining hematopoietic stem cell function. DNA Repair (Amst) 7 (3), 523–529. http://dx.doi.org/10.1016/j.dnarep.2007.11.012 (S1568-7864(07)00413-2 [pii]).

Pace, P., Mosedale, G., Hodskinson, M.R., Rosado, I.V., Sivasubramaniam, M., Patel, K.J., 2010. Ku70 corrupts DNA repair in the absence of the Fanconi anemia pathway. Science 329 (5988), 219–223. http://dx.doi.org/10.1126/science.1192277 (science.1192277 [pii]).

Parmar, K., D'Andrea, A., Niedernhofer, L.J., 2009. Mouse models of Fanconi anemia. Mutat. Res. 668 (1–2), 133–140. http://dx.doi.org/10.1016/j.mrfmmm.2009.03.015 (S0027-5107(09)00117-1 [pii]).

Raya, A., Rodriguez-Piza, I., Guenechea, G., Vassena, R., Navarro, S., Barrero, M.J., Consiglio, A., Castella, M., Rio, P., Sleep, E., Gonzalez, F., Tiscornia, G., Garreta, E., Aasen, T., Veiga, A., Verma, I.M.,

Surralles, J., Bueren, J., Izpisua Belmonte, J.C., 2009. Disease-corrected haematopoietic progenitors from Fanconi anaemia induced pluripotent stem cells. Nature 460 (7251), 53–59. http://dx.doi.org/10.1038/nature08129 (nature08129 [pii]).

Rocha, C.R., Lerner, L.K., Okamoto, O.K., Marchetto, M.C., Menck, C.F., 2013. The role of DNA repair in the pluripotency and differentiation of human stem cells. Mutat. Res. (1), 25–35. http://dx.doi.org/10.1016/j.mrrev.2012.09.001 (S1383-5742(12)00061-0 [pii]).

Sasaki, M.S., Tonomura, A., 1973. A high susceptibility of Fanconi's anemia to chromosome breakage by DNA cross-linking agents. Cancer Res. 33 (8), 1829–1836.

Schindler, D., Hoehn, H., 1988. Fanconi anemia mutation causes cellular susceptibility to ambient oxygen. Am. J. Hum. Genet. 43 (4), 429–435.

Song, H., Chung, S.K., Xu, Y., 2010. Modeling disease in human ESCs using an efficient BAC-based homologous recombination system. Cell Stem Cell 6 (1), 80–89. http://dx.doi.org/10.1016/j.stem.2009.11.016 (S1934-5909(09)00623-7 [pii]).

Tulpule, A., Lensch, M.W., Miller, J.D., Austin, K., D'Andrea, A., Schlaeger, T.M., Shimamura, A., Daley, G.Q., 2010. Knockdown of Fanconi anemia genes in human embryonic stem cells reveals early developmental defects in the hematopoietic lineage. Blood 115 (17), 3453–3462. http://dx.doi.org/10.1182/blood-2009-10-246694 (blood-2009-10-246694 [pii]).

Utikal, J., Polo, J.M., Stadtfeld, M., Maherali, N., Kulalert, W., Walsh, R.M., Khalil, A., Rheinwald, J.G., Hochedlinger, K., 2009. Immortalization eliminates a roadblock during cellular reprogramming into iPS cells. Nature 460 (7259), 1145–1148. http://dx.doi.org/10.1038/nature08285 (nature08285 [pii]).

Waisfisz, Q., Morgan, N.V., Savino, M., de Winter, J.P., van Berkel, C.G., Hoatlin, M.E., Ianzano, L., Gibson, R.A., Arwert, F., Savoia, A., Mathew, C.G., Pronk, J.C., Joenje, H., 1999. Spontaneous functional correction of homozygous Fanconi anaemia alleles reveals novel mechanistic basis for reverse mosaicism. Nat. Genet. 22 (4), 379–383. http://dx.doi.org/10.1038/11956.

Yao, Y., Nashun, B., Zhou, T., Qin, L., Zhao, S., Xu, J., Esteban, M.A., Chen, X., 2012. Generation of CD34+ cells from CCR5-disrupted human embryonic and induced pluripotent stem cells. Hum. Gene Ther. 23 (2), 238–242. http://dx.doi.org/10.1089/hum.2011.126.

Yung, S.K., Tilgner, K., Ledran, M.H., Habibollah, S., Neganova, I., Singhapol, C., Saretzki, G., Stojkovic, M., Armstrong, L., Przyborski, S., Lako, M., 2013. Brief report: human pluripotent stem cell models of Fanconi anemia deficiency reveal an important role for Fanconi anemia proteins in cellular reprogramming and survival of hematopoietic progenitors. Stem Cells 31 (5), 1022–1029. http://dx.doi.org/10.1002/stem.1308.

Zhang, S., Yajima, H., Huynh, H., Zheng, J., Callen, E., Chen, H.T., Wong, N., Bunting, S., Lin, Y.F., Li, M., Lee, K.J., Story, M., Gapud, E., Sleckman, B.P., Nussenzweig, A., Zhang, C.C., Chen, D.J., Chen, B.P., 2011. Congenital bone marrow failure in DNA-PKcs mutant mice associated with deficiencies in DNA repair. J. Cell Biol. 193 (2), 295–305. http://dx.doi.org/10.1083/jcb.201009074 (jcb.201009074 [pii]).